Surface & Coatings Technology 276 (2015) 602–605

Contents lists available at ScienceDirect

Surface & Coatings Technology

journal homepage: www.elsevier.com/locate/surfcoat

First-principles study of W–TiC interface cohesion

D.Y. Dang, L.Y. Shi, J.L. Fan, H.R. Gong *

State Key Laboratory of Powder Metallurgy, Central South University, Changsha, Hunan 410083, China

ARTICLE INFO

Article history:
Received 6 April 2015
Revised 3 June 2015
Accepted in revised form 5 June 2015
Available online 8 June 2015

Keywords:
First principles calculation
W–TiC interface
Work of separation
Interface energy

ABSTRACT

First principles calculation reveals that the W–TiC interfaces with one overlayer possess high interface strength and are thermodynamically stable with negative interface energies, which could serve as the driving force for interdiffusion of W and TiC. It is also found that interface orientation should have an important effect on interface cohesion, *i.e.*, the W(110)–TiC(100) interfaces are not only energetically more favorable with lower interface energies, but also possess higher interface strength than the corresponding W(100)–TiC(100) interfaces, suggesting that the W(110)–TiC(100) interfaces should be more preferred in actual applications. Moreover, the electronic structures would give a deep understanding of cohesion properties of various W–TiC interfaces, and the derived results agree well with experimental observations in the literature.

1. Introduction

The W–TiC system has raised great research interests during the past years [1–13]. First of all, TiC particles have been widely added, as reinforcements and grain refiners, to improve the mechanical properties of W matrix for high temperature applications, such as structural components in fusion devices and specimen grips during high temperature testing [1,2,5–8]. Moreover, the TiC–W clad layer has been deposited on steel to enhance its wear resistance [11,12], and epitaxial TiC/W multilayers could be promising quantum well devices due to their unique mechanical, electrical, and optical properties [9,10]. In addition, an intermediate W layer has been placed between TiC protection layer and molybdenum substrate, in order to improve the thermal stability of TiC–Mo interface for fusion reactor first wall applications [13].

It is well known that the cohesion properties of TiC/W interfaces play a very important role in the performance of various TiC–W products. Several experimental studies have qualitatively shown that the interface cohesion between TiC and W seems good [2,7–9], and that a (Ti, W)C solid solution transition zone could be formed in the W–TiC interface [2,7,8]. Nevertheless, no detailed interface properties of TiC/W have been reported so far in the literature, and the fundamental mechanism of TiC/W interface cohesion also needs further theoretical investigation.

By means of highly accurate total energy calculations based on density functional theory [14,15], the present study is, therefore, dedicated to find out the interface strength and interface energy of several W–TiC interfaces. The derived results will be compared extensively with experimental evidence in the literature, and the fundamental mechanism will be revealed in terms of electronic structures, which could provide a deep understanding to various interface properties of W–TiC.

2. Method of calculation

The present first-principles calculation is based on the well-established Vienna *ab initio* simulation package (VASP) with the projector-augmented wave (PAW) method [16]. The exchange and correlation items are described by generalized gradient approximation (GGA) of Perdew et al. [17], and the cutoff energy is 500 eV for plane-wave basis. The interface calculations are focused on four interface structures, *i.e.*, W(100)/TiC(100), TiC(100)/W(100), W(110)/TiC(100), and TiC(100)/W(110), in which the first and second parts are overlayer and substrate, respectively. The optimized bulk lattice constants of the substrates and its crystal structures, *i.e.*, 3.176 Å of BCC and 4.339 Å of the rock-salt structure, are chosen for W- and TiC-based interfaces, respectively [4,18].

To achieve a good lattice match, a 1×1 surface unit cell is selected for both W(100) and TiC(100) in the W(100)/TiC(100) and TiC(100)/W(100) interfaces, while 1×2 for W(110) and 1×3 for TiC(100) in the W(110)/TiC(100) and TiC(100)/W(110) interfaces. Before the interface calculation, a series of surface tests have been performed for the ground-state structures of W (BCC) and TiC (rock-salt). The number of surface layers is gradually increased until the surface energy convergence is reached with a criterion of 0.01 J/m^2, and the thickness of vacuum layers is also tested in a similar way to get converged surface energy and work function. Based on these tests, 7 substrate layers with a vacuum layer of 20 Å are selected for each interface before adding a certain number (1–5) of overlayers at the top of the substrate layers.

* Corresponding author.
E-mail address: gonghr@csu.edu.cn (H.R. Gong).

http://dx.doi.org/10.1016/j.surfcoat.2015.06.009
0257-8972/

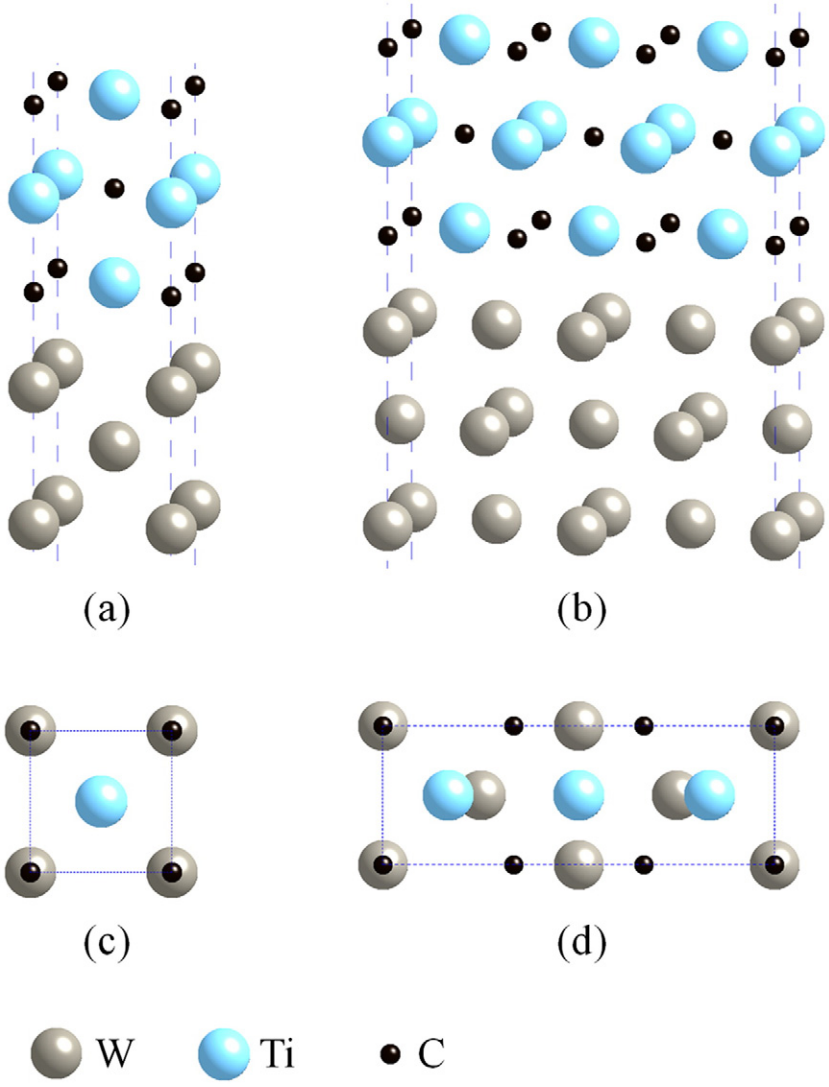

Fig. 1. Three dimensional atomic configurations of (a) TiC(100)/W(100) and (b) TiC(100)/W(110) interfaces. (c) and (d) are top views of the interfacial atoms corresponding to (a) and (b), respectively.

As typical examples, Fig. 1 shows the atomic configurations of TiC(100)/W(100) and TiC(100)/W(110) interfaces. It should be pointed out that the above interface settings are just to simulate the experimental epitaxial growth of TiC/W multilayers [9], and that the lattice mismatches of the present interface models are very small values of less than 3.5% with in-plane periodicity.

In each calculation, periodic boundary conditions are added in three directions of the unit cell, and the Gamma centered *k* grid is adopted, *i.e.*, $11 \times 11 \times 1$ and $11 \times 4 \times 1$ for W(100)–TiC(100) and W(110)–TiC(100) interfaces, respectively, within both relaxation and static calculations; while $21 \times 21 \times 1$ and $21 \times 7 \times 1$ for density of states (DOS) calculations of W(100)–TiC(100) and W(110)–TiC(100) interfaces, respectively. Energy criteria are 0.01 and 0.001 meV for relaxation and static calculations, respectively.

3. Results and discussion

Before the interface calculation, the surface properties have been obtained for W(100), W(110), and TiC(100) surfaces. It is found that the calculated results from the present study agree well with the available results in the literature [19,20]. For instance, the surface energies of W(100) and W(110) from the present study are 3.904 and 3.212 J/m^2, respectively, with an average value of 3.558 J/m^2, which matches well with the corresponding experimental values of 3.675 J/m^2 [19]. The work function of TiC(100) is calculated to be 4.643 eV, which is also compatible with the corresponding data of 4.1 eV from experiments [20]. Moreover, a surface undulation of TiC(100) after relaxation has been observed in the present study, *i.e.*, the outward relaxation of 1.5% for C and the inward relaxation of 3.7% for Ti. It should be noted that such a relaxation tendency of Ti and C is in good accordance with experimental and theoretical results [21–23].

The work of separation (W_{sep}) of W–TiC interfaces is first calculated through the following formula:

$$W_{sep} = \frac{E_W + E_{TiC} - E_{tot}}{2A}, \tag{1}$$

where E_{tot} and A are total energy and interface area of the W–TiC interface, respectively, and E_W and E_{TiC} correspond to total energies of pure W and TiC surface layers after the removal of the TiC and W layers, respectively. It should be noted that W_{sep} is the reversible work needed to separate the interface into two free surfaces, and therefore a direct measure of the interface bond strength. Consequently, the W_{sep} values of the four W–TiC interfaces are derived and shown in Fig. 2(a). It can be seen that each W–TiC interface has very high interface strength, and that the highest interface strength is reached for each interface

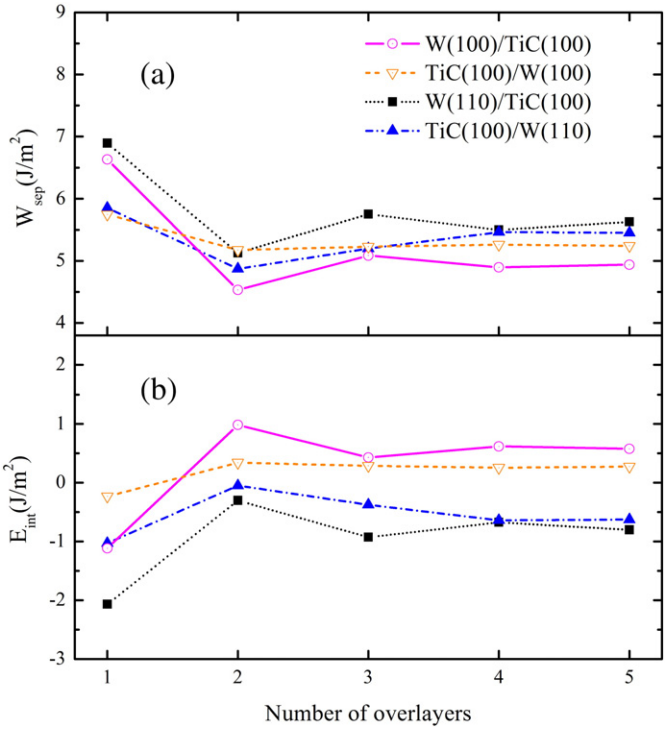

Fig. 2. (a) Work of separation (W_{sep}) and (b) interface energy (E_{int}) of W–TiC interfaces.

when the number of overlayers is one. Moreover, the interface orientation plays an important role in interface strength, *i.e.*, the descending sequence of W_{sep} of W–TiC interfaces with five overlayers is as follows: W(110)/TiC(100) → TiC(100)/W(110) → TiC(100)/W(100) → W(100)/TiC(100). Interestingly, the W_{sep} of W(110)–TiC(100) interfaces with five overlayers is generally bigger than that of the W(100)–TiC(100) interfaces, suggesting that the W(110) surface has stronger cohesion with the TiC(100) surface than W(100).

To find out the thermodynamics of the W–TiC interface, the interface energy (E_{int}) is then calculated according to the following form:

$$E_{\text{int}} = \frac{E_{tot} - E_{bulk\_W} - E_{bulk\_TiC}}{2A}, \quad (2)$$

where E_{bulk_W} and E_{bulk_TiC} are bulk energies of the W and TiC layers, respectively. Fundamentally, the interface energy can be defined as the energy of interface formation by means of two bulk phases, and is therefore an expression of interface stability. Accordingly, the calculated interface energies of the four interfaces are displayed in Fig. 2(b). It can be discerned from Fig. 2(b) that each interface with one overlayer has the lowest and negative E_{int} value, which is consistent with the highest interface strength shown in Fig. 2(a). One could also see that the W(110)–TiC(100) interfaces have much lower E_{int} values than the W(100)–TiC(100) interfaces, implying that the W(110)–TiC(100) interfaces should be energetically more favorable and thermally more stable. As shown in Fig. 2, both W_{sep} and E_{int} values of the four interfaces have converged with the number of overlayers, while very small fluctuation could be seen in the W(100)/TiC(100) and W(110)/TiC(100) interfaces, and such kind of fluctuation would be probably attributed to the well-known quantum size effect [24].

It is of interest to compare the above calculated results with available experimental evidence in the literature. Firstly, the high W_{sep} values of W–TiC interfaces shown in Fig. 2 suggest that the W–TiC interfaces possess high interface strength and that the interface cohesion between W and TiC should be strong, which agrees well with similar experimental observations in the literature [2,7–9]. Such high interface strength could ensure the load transferring of W–TiC interfaces and be responsible for the strengthening effect of TiC dispersed W matrix and W–TiC multilayers [2,7,10].

Secondly, the negative E_{int} values of the four W–TiC interface with one overlayer shown in Fig. 2(b) imply that the interdiffusion between W and TiC could happen in the interface region, which is in excellent agreement with the interdiffusion zone (solid solution transition zone) at W–TiC interfaces observed from experiments [2,7,8]. In other words, it is the negative interface energy which fundamentally induces the interface interdiffusion of W–TiC interfaces.

Thirdly, both W_{sep} and E_{int} values of W(100)/TiC(100) and TiC(100)/W(100) interfaces with five overlayers are close to each other. A similar feature could be also observed for W(110)/TiC(100) and TiC(100)/W(110) interfaces. Such a similarity of interface strength and interface energy suggests that the strain effect within the W–TiC interfaces should be very small, which is compatible with the experimentally epitaxial growth of W–TiC mutilayers [9].

Fourthly, it can be seen from Fig. 2(b) that the interface energies of both W(100)–TiC(100) interfaces are very close to zero, suggesting that the W(100)/TiC(100) and TiC(100)/W(100) interfaces should be thermodynamically favorable and could possibly be formed in real situation, which is consistent with the experimental observation of the W(100)–TiC(100) multilayers [9].

We discuss a little bit more about the interface cohesion of W–TiC. As shown in Fig. 2 related before, the W(110)–TiC(100) interfaces with five overlayers are not only energetically more favorable with lower interface energies, but also possess higher interface strength than the corresponding W(100)–TiC(100) interfaces. Such a comparison implies that interface orientation should have an important effect on interface cohesion of W–TiC, and that the W(110)–TiC(100) interfaces are more preferred in actual applications. It should be pointed out that the W(110)–TiC(100) interfaces have not been reported

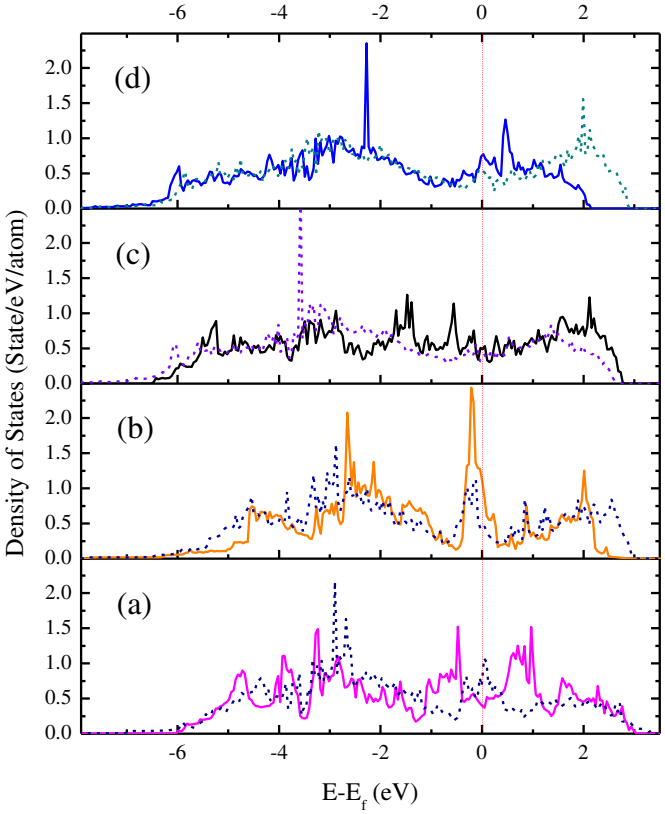

Fig. 3. Total density of states (DOS) of interfacial atoms in (a) W(100)/TiC(100), (b) TiC(100)/W(100), (c) W(110)/TiC(100), and (d) TiC(100)/W(110) interfaces. The solid and dashed lines are for interfaces with one and five overlayers, respectively.

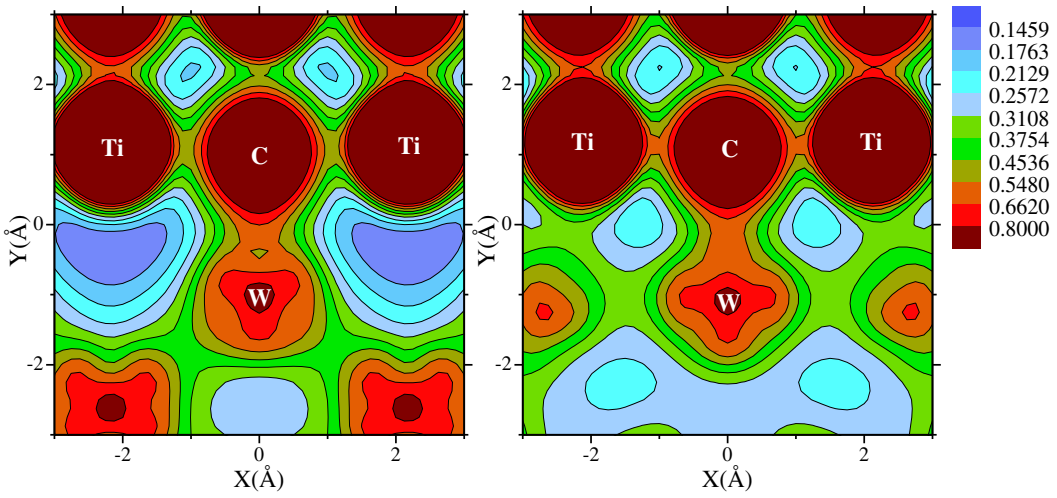

Fig. 4. Charge density plots of (a) W(100)/TiC(100) and (b) W(110)/TiC(100) interfaces with five overlayers. The charge density is in the unit of e/Å^3.

experimentally so far in the literature, and further experimental studies are therefore needed to confirm the W(110)–TiC(100) interfaces.

To have a deep understanding of interface cohesion from the perspective of electronic structure, Fig. 3 shows the comparison of total density of states (DOS) of each interfaces with one and five overlayers. It is clear from this figure that compared with the model with five overlayers, each interface with one overlayer possesses a smaller bandwidth of DOS, and the electronic structure is more localized with higher values of DOS peaks near the Fermi level. Such comparison implies that each interface with one overlayer should have a stronger chemical bonding, which would therefore induce the higher interface strength and lower interface energy as displayed in Fig. 2.

In addition, Fig. 4, as another example, displays the comparison of charge densities of W(100)/TiC(100) and W(110)/TiC(100) interfaces with five overlayers. One can observe clearly from Fig. 4 that the charge densities from the interfacial W to C in both W(100)/TiC(100) and W(110)/TiC(100) interfaces are directional and dense, suggesting that a pronounced covalent bond has been formed between interfacial W and C atoms. Such a strong W–C bond should therefore cause the good interface cohesion of W–TiC as related before. Furthermore, a careful observation would reveal that the charge densities within the interface region of W(110)/TiC(100) seem a little bit denser than those of W(100)/TiC(100), which could thus bring about a deep understanding to the stronger interface cohesion of W(110)/TiC(100) as shown in Fig. 2.

4. Concluding remarks

First principles calculation has been conducted to reveal interface bond strength and interface energy of various W–TiC interfaces. It is found that interface orientation and the number of overlayers play important roles in interface cohesion of W–TiC. The thermodynamically more stable interface configuration of W(110)–TiC(100) is first proposed to have a better interface cohesion than the experimental observed configuration of W(100)–TiC(100). The density of states (DOS) and charge densities are given for further understanding of various interface properties, and the derived results are in good agreement with experimental observations.

Acknowledgments

This research work is supported by Research of ITER Tungsten Divertor Technology (No.: 2011GB110002), Key Project of ITER of Ministry of Science and Technology of China (No.: 2014GB115000), and the Fundamental Research Funds for the Central Universities of Central South University (No.: 2015zzts182).

References

[1] S.W. Yih, C.T. Wang, Tungsten: Sources, Metallurgy, Properties, and Applications, Plenum Press, New York, 1979.
[2] Y. Chen, Y.C. Wu, F.W. Yu, J.L. Chen, Int. J. Refract. Met. Hard Mater. 26 (2008) 525.
[3] Q.Q. Ren, J.L. Fan, Y. Han, H.R. Gong, J. Appl. Phys. 116 (2014) 093909;
C. Wei, J.L. Fan, H.R. Gong, J. Alloys Compd. 618 (2015) 615.
[4] D.Y. Dang, J.L. Fan, H.R. Gong, J. Appl. Phys. 116 (2014) 033509.
[5] X. Liu, J. Chen, Y. Lian, J. Wu, Z. Xu, N. Zhang, Q. Wang, X. Duan, Z. Wang, J. Zhong, J. Nucl. Mater. 442 (2013) S309.
[6] H. Kurishita, Y. Amano, S. Kobayashi, K. Nakai, H. Arakawa, Y. Hiraoka, T. Takida, K. Takebe, H. Matsui, J. Nucl. Mater. 367–370 (2007) 1453 (Part B).
[7] G.M. Song, Y.J. Wang, Y. Zhou, Int. J. Refract. Met. Hard Mater. 21 (2003) 1.
[8] G.M. Song, Y. Zhou, Y.J. Wang, J. Mater. Sci. 37 (2002) 3541.
[9] J.L. He, W.Z. Li, Jan, J. Appl. Phys. 37 (1998) L679.
[10] J.L. He, W.Z. Li, H.D. Li, C.H. Liu, Surf. Coat. Technol. 103–104 (1998) 276.
[11] S.W. Wang, Y.C. Lin, Y.Y. Tsai, J. Mater. Process. Technol. 140 (2003) 682.
[12] Y.C. Lin, S.W. Wang, Wear 256 (2004) 720.
[13] M. Fukutomi, M. Fujitsuka, T. Shikama, M. Okada, J. Vac. Sci. Technol. A 3 (1985) 2650.
[14] J.W. Wang, H.R. Gong, Int. J. Hydrogen Energy 39 (2014) 1888.
Int. J. Hydrogen Energ. 39 (2014) 6068.
[15] C.P. Liang, H.R. Gong, Mater. Lett. 115 (2014) 252;
J.W. Wang, Y.H. He, H.R. Gong, J. Membr. Sci. 475 (2015) 406.
[16] G. Kresse, D. Joubert, Phys. Rev. B 59 (1999) 1758.
[17] J.P. Perdew, J. Chevary, S. Vosko, K.A. Jackson, M.R. Pederson, D. Singh, C. Fiolhais, Phys. Rev. B 46 (1992) 6671.
[18] Q.Q. Ren, D.Y. Dang, H.R. Gong, J.L. Fan, Y.M. Zhao, Carbon 83 (2015) 100;
Q.Q. Ren, J.L. Fan, H.R. Gong, Mater. Lett. 145 (2015) 205.
[19] F.R. deBoer, R. Boom, W.C.M. Mattens, A.R. Miedema, A.K. Niessen, Cohesion in Metals: Transition Metal Alloys, North-Holland, Amsterdam, 1989.
[20] P.A.P. Lindberg, L.I. Johansson, Surf. Sci. 194 (1988) 199.
[21] S. Bağcı, T. Kamış, H. Tütüncü, G. Srivastava, Phys. Rev. B 80 (2009) 035405.
[22] D.L. Price, J.M. Wills, B.R. Cooper, Phys. Rev. Lett. 77 (1996) 3375.
[23] J.A. Rodriguez, P. Liu, J. Dvorak, T. Jirsak, J. Gomes, Y. Takahashi, K. Nakamura, J. Chem. Phys. 121 (2004) 465.
[24] Y. Han, D.J. Liu, Phys. Rev. B 80 (2009) 155404.